

# Preparation of dense spherical Ni particles and hollow NiO particles by spray pyrolysis

S.-L. CHE, K. TAKADA

*Electronics Business Division, Sumitomo Metal Mining Co., Ltd, 1-6-1, Suehiro-cho, Ome-shi, Tokyo 198, Japan*

*E-mail: che@sim.ceram.titech.ac.jp*

K. TAKASHIMA, O. SAKURAI, K. SHINOZAKI, N. MIZUTANI\*

*Department of Inorganic Materials, Faculty of Engineering, Tokyo Institute of Technology 2-12-1, O-okayama, Meguro-ku, Tokyo 152, Japan*

Dense spherical Ni particles were prepared from nitrate solution by spray pyrolysis in a  $H_2$ - $N_2$  atmosphere. Hollow NiO particles with rough surfaces were formed first at low temperature and then reduced to Ni by  $H_2$  above 300 °C. Subsequent intraparticle sintering of the Ni crystallites gave rise to densification of Ni particles as the temperature was raised; most Ni particles became dense above the pyrolysis temperature of 1000 °C. However, when a  $N_2$  atmosphere was used, hollow NiO particles were formed, which did not densify even at 1200 °C due to the lack of sintering. The dense Ni particles obtained were of good crystallinity and good oxidation resistance, especially for those formed at higher pyrolysis temperatures and longer residence times. © 1999 Kluwer Academic Publishers

## 1. Introduction

The continuous demand for size reduction and capacitance increase of multilayer ceramic capacitors (MLC) has been requesting the increase of layer numbers and the thinning of dielectric layers and internal electrodes. One of the biggest obstacles to this trend is the set-up cost, due to increased use of noble metals to form internal electrodes. In recent years, development of new dielectric materials that can be sintered in a reductive atmosphere enabled the use of cheap metal electrodes, such as nickel, instead of noble metals [1]. It is clear that Ni will replace Pd to become the most important electrode material for multilayer components before the year 2000. Ni powders for this use have been mainly produced by wet chemical precipitation [2] or gas phase reaction [3]. However, Ni powders of good crystallinity, spherical shape and uniform size distribution for good film-forming performance [2, 4] are very difficult to obtain by these methods.

Spray pyrolysis is a useful method for the preparation of spherical particles of oxide, metal, non-oxide and even polymer [5]. Very high homogeneity can be obtained even for powders of very complex composition. However, rapid evaporation of solvent and dramatic evolution of decomposition gases from the droplets/particles make it very difficult to control the particle structure. In many cases hollow or irregular shaped particles are formed. It is realized that the structure of particle is determined by processes like the precipitation of solids from droplets, intradroplet reactions, evolution of gases, intraparticle reactions and

intraparticle sintering, etc. [6]. The most important operating factors include the property of the starting material, the concentration of the solution, the drying and pyrolysis temperatures, the residence time and heating rate of the droplets/particles. Normally, preparation conditions of a flat temperature profile and sufficient heating time are advantageous to the formation of dense particles.

Preparation of metal powders by spray pyrolysis has been receiving intensive research interest in this decade [7, 8]. Nagashima *et al.* reported the formation of spherical metal particles, such as Ni, Cu, Pd and Ag, by spray pyrolysis. However, the particles were hollow below the melting point and dense metal particles were obtained only above the melting point [8]. In previous studies we have prepared dense and single-crystal spherical palladium particles by spray pyrolysis [9, 10]. For Ni powder, a reductive atmosphere is necessary and nitrate is preferred to chloride as the starting material [8, 11]. In this paper, we report the formation of dense single-crystal-like Ni particles below the melting point by spray pyrolysis and the evolution of particle structure in the process.

## 2. Experimental procedure

### 2.1. Powder preparation

Ni powders were prepared from a  $1.0 \text{ mol dm}^{-3}$  aqueous solution of  $Ni(NO_3)_2 \cdot 6H_2O$  (special pure agent, Wako) solution. The synthesis apparatus [12] was composed of an ultrasonic atomizer (approximately

\* Author to whom correspondence should be addressed.

1.7 MHz); a horizontal reaction tube (alumina, 50 mm internal diameter and 2000 mm in length), which was heated by two electric furnaces set at  $T_1$  and  $T_2$ , respectively, for the drying of droplets and the pyrolysis of solid particles; and a filtration system for collecting the formed particles. Temperatures of the furnaces were varied in the range  $T_1 = 200\text{--}600\text{ }^\circ\text{C}$  and  $T_2 = 400\text{--}1400\text{ }^\circ\text{C}$ . A mixed gas containing 15%  $\text{H}_2$  and 85%  $\text{N}_2$  was used as the carrier gas to make a reductive atmosphere and the gas flow rate was varied between 0.8 and  $4.0\text{ cm s}^{-1}$  (residence time 30–150 s in the hot zone). The main runs of preparations were carried out at  $T_1 = 400\text{ }^\circ\text{C}$ ,  $T_2 = 1200\text{ }^\circ\text{C}$  at a gas flow rate of  $3.0\text{ cm s}^{-1}$ .

## 2.2. Characterization

Morphological features of the particles were observed in the uncoated state with a field emission scanning electron microscope (SEM, Hitachi S-800). An X-ray diffractometer (XRD, Philips PW1700) was used for phase analysis of the prepared powders. Crystallite sizes of the powders were determined by the XRD line-broadening method. Oxygen content was measured with an oxygen–nitrogen analyser (Leco TC-136). Specific surface areas (SSA) of the powders were measured by Bronauer–Emmett–Teller (BET) nitrogen adsorption (Micromeritics Flowsorb II 2300). Particle density was measured by means of an automatic gas pycnometer (Micromeritics Accupyc 1330), with He as the working gas. To investigate the internal structure of the particles [12], a powder was embedded into an epoxy resin and then sliced to 40–80 nm in thickness by ultramicrotomy (Reichert-Nissei Ultracut N). Microtome sections were observed with a transmission electron microscope (TEM, Jeol JEM-200CX). Thermal analysis (thermogravimetric–differential thermal analysis; TGA–DTA, Rigaku TAS-200) was carried out at a heating rate of  $10\text{ }^\circ\text{C min}^{-1}$  in air atmosphere to investigate the oxidation behaviour of the Ni powders.

## 3. Results and discussion

### 3.1. Morphology of the particles

XRD analysis showed that the powders prepared in the nitrogen atmosphere or below the pyrolysis temperatures of  $T_2 = 400\text{ }^\circ\text{C}$  in the  $\text{H}_2\text{--N}_2$  atmosphere were composed of NiO. Particles obtained above the pyrolysis temperature of  $T_2 = 600\text{ }^\circ\text{C}$  in the  $\text{H}_2\text{--N}_2$  atmosphere were single-phase cubic Ni. Oxygen contents of the Ni powders were around 0.2 mass %, less than the normal surface oxidation level of 1 mass % for Ni powders produced by other methods. Crystallite size of the Ni particles increased with rising  $T_2$ . A crystallite size of around 50 nm was obtained at  $T_2 = 800\text{ }^\circ\text{C}$ , but above  $T_2 = 1000\text{ }^\circ\text{C}$  the crystallite sizes exceeded the measurable range of the XRD line-broadening method (about 200 nm). This indicates that the Ni crystallite sizes were increased to the same order as the particle size and most of the Ni particles were nearly single crystal.

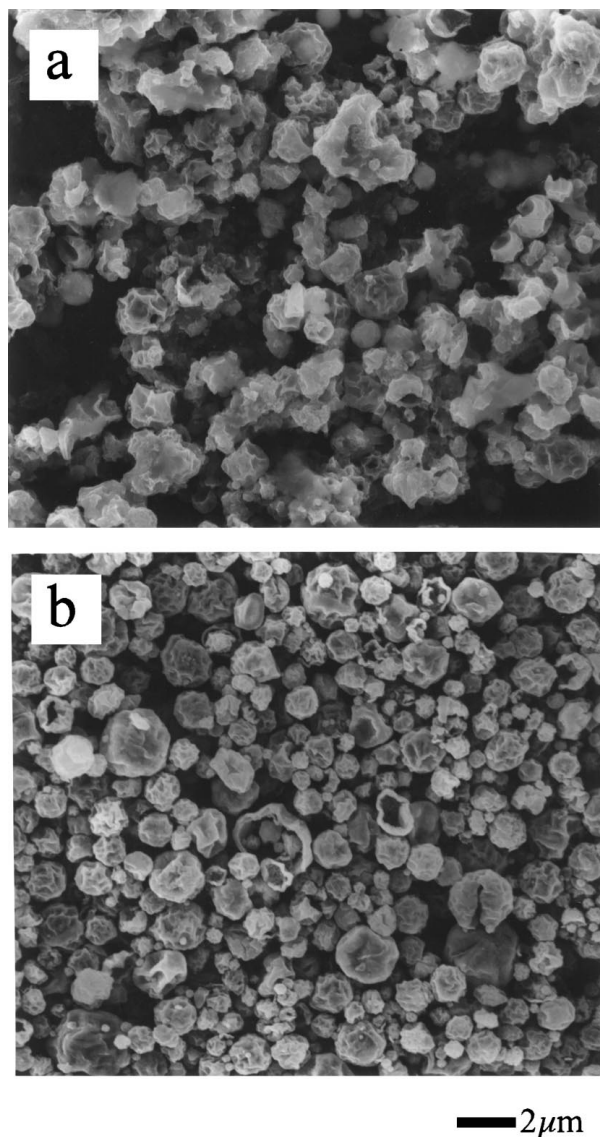


Figure 1 SEM photographs showing the morphologies of NiO particles prepared at (a)  $T_1 = 200\text{ }^\circ\text{C}$ ,  $T_2 = 400\text{ }^\circ\text{C}$ ; and (b)  $T_1 = 400\text{ }^\circ\text{C}$ ,  $T_2 = 1200\text{ }^\circ\text{C}$  in  $\text{N}_2$  atmosphere and a carrier gas flow rate of  $3.0\text{ cm s}^{-1}$ .

Fig. 1 shows SEM photographs of the NiO particles prepared at different pyrolysis temperatures in the  $\text{N}_2$  atmosphere. Fragments of shells observed in the SEM photographs showed the existence of hollow particles, which had been indicated by TEM observation shown in Fig. 2. Most of the NiO particles were deformed with many depressions on the particle surfaces, possibly owing to the non-uniform shrinkage of the hollow particles when they were cooled to room temperature in the preparation process.

Fig. 3 shows SEM photographs of the Ni particles prepared at different pyrolysis temperatures in the  $\text{H}_2\text{--N}_2$  atmosphere. Ni particles formed below  $T_2 = 800\text{ }^\circ\text{C}$  had similar morphology to the NiO particles but were more spherical, with rough surfaces and a fraction of irregular-shaped particles. However, at  $T_2 = 1000\text{--}1400\text{ }^\circ\text{C}$ , almost all Ni particles were ideal spheres with smooth and dense surfaces. The decrease of particle size at higher  $T_2$  (Fig. 3) is attributed to the densification of Ni particles and the decrease of large hollow particles.

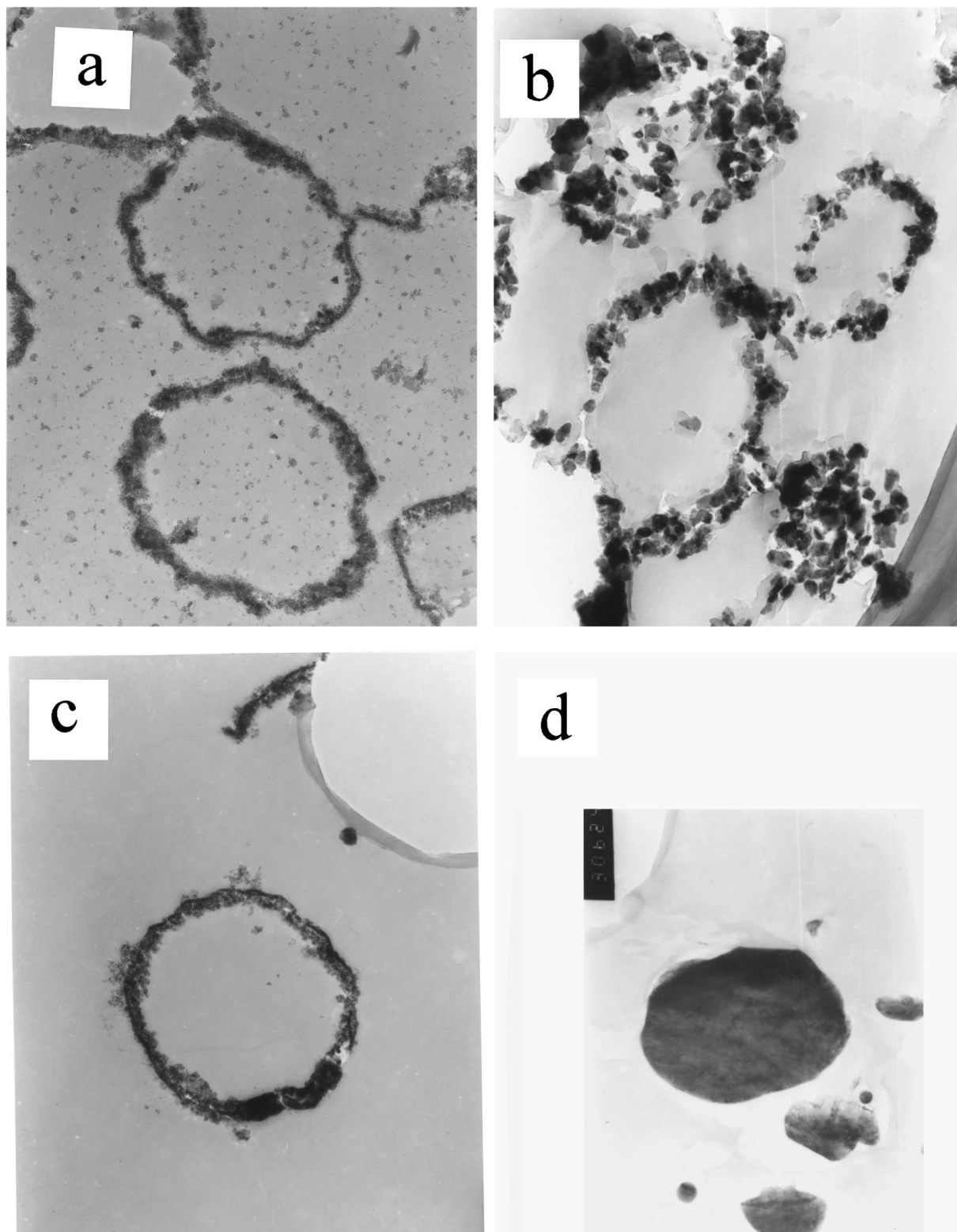


Figure 2 TEM micrographs of the microtome sections of the particles prepared at various conditions. (a) NiO powder prepared at  $T_1 = 200\text{ }^\circ\text{C}$ ,  $T_2 = 400\text{ }^\circ\text{C}$ ,  $\text{N}_2$  atmosphere; (b) NiO powder prepared at  $T_1 = 400\text{ }^\circ\text{C}$ ,  $T_2 = 1200\text{ }^\circ\text{C}$ ,  $\text{N}_2$  atmosphere; (c) powder containing Ni and NiO, prepared at  $T_1 = 200\text{ }^\circ\text{C}$ ,  $T_2 = 400\text{ }^\circ\text{C}$ ,  $\text{H}_2\text{-N}_2$  atmosphere; (d) Ni powder prepared at  $T_1 = 400\text{ }^\circ\text{C}$ ,  $T_2 = 1200\text{ }^\circ\text{C}$ ,  $\text{H}_2\text{-N}_2$  atmosphere.

A decrease of the fraction of large and irregular particles with the decrease of carrier gas flow rate was confirmed by SEM observation of the Ni particles. As a result, the width of the particle size distribution was decreased. This is attributed to the increase

of residence time and the decrease of heating rate for the particles at slower gas flow rates. However, little difference was found between the particle morphologies when the drying temperature was varied in the range  $T_1 = 300\text{--}600\text{ }^\circ\text{C}$ .

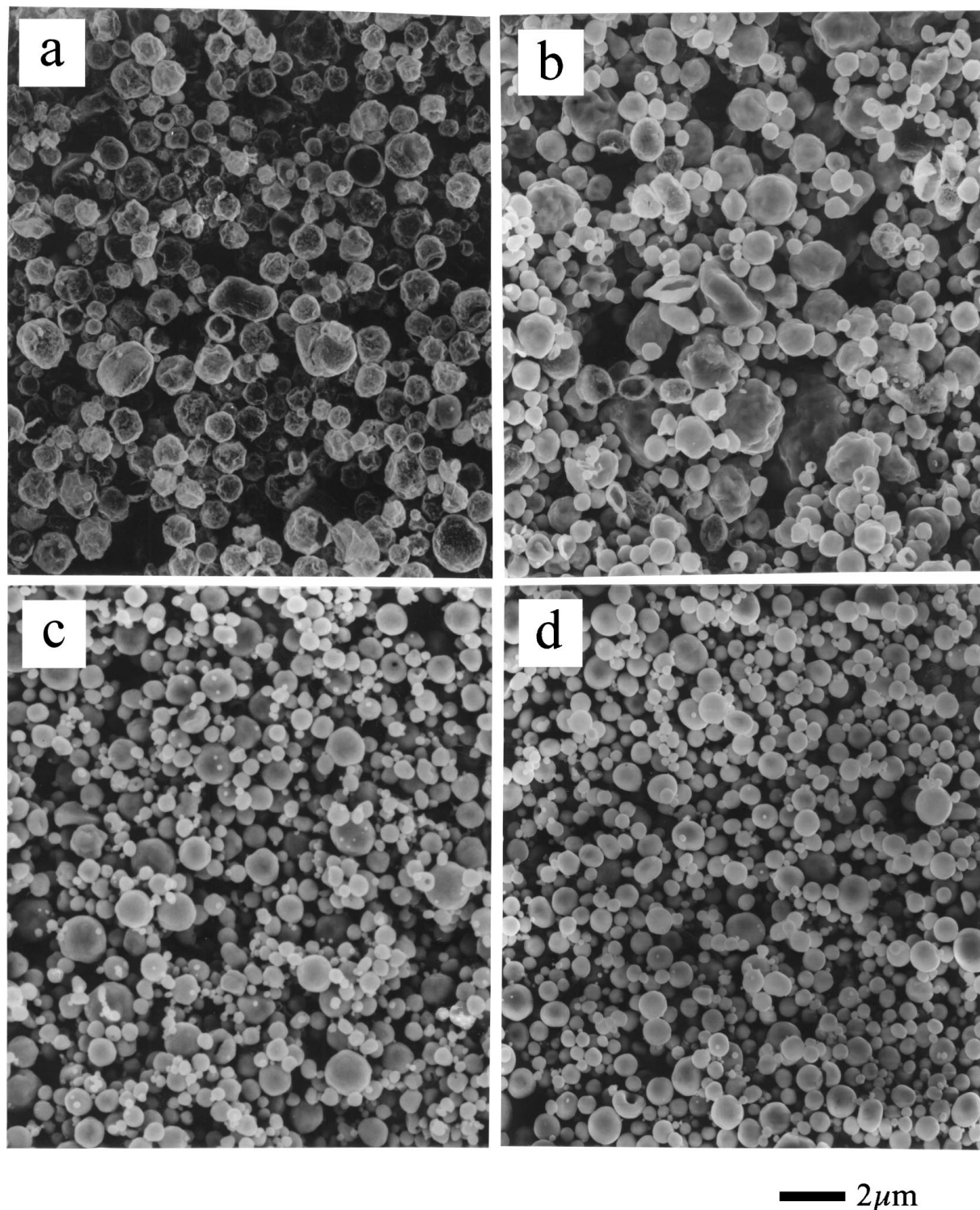


Figure 3 SEM photographs showing the morphologies of Ni particles prepared at (a)  $T_1 = 200\text{ }^\circ\text{C}$ ,  $T_2 = 400\text{ }^\circ\text{C}$  (containing a little NiO); (b)  $T_1 = 400\text{ }^\circ\text{C}$ ,  $T_2 = 800\text{ }^\circ\text{C}$ ; (c)  $T_1 = 400\text{ }^\circ\text{C}$ ,  $T_2 = 1000\text{ }^\circ\text{C}$ ; and (d)  $T_1 = 400\text{ }^\circ\text{C}$ ,  $T_2 = 1200\text{ }^\circ\text{C}$  in  $\text{H}_2\text{-N}_2$  atmosphere at a carrier gas flow rate of  $3.0\text{ cm s}^{-1}$ .

### 3.2. Evolution of internal structure of the particles

It is believed that when a droplet of  $\text{Ni}(\text{NO}_3)_2$  solution is heated, a dried-salt particle of  $\text{Ni}(\text{NO}_3)_2$  is formed, because it does not hydrolyse to form a hydroxide or hydroxynitrate precipitate. At about  $300\text{ }^\circ\text{C}$ ,  $\text{Ni}(\text{NO}_3)_2$  decomposes to form NiO [13], which is further reduced to Ni by  $\text{H}_2$  at higher temperature. In this way, the structure of a particle is determined by (i) the drying of a droplet, (ii) the reduction of NiO to Ni, and (iii) the sintering of Ni crystallites formed within a particle.

Fig. 2 shows TEM photographs of microtome sections of NiO and Ni particles prepared at different conditions. Consistent with SEM observations (Figs 1 and 3), all NiO particles formed in the nitrogen atmosphere, even at the pyrolysis temperature of  $1200\text{ }^\circ\text{C}$ , were hollow and composed of nanometre-sized crystallites of NiO (Fig. 2a, b). No structural change, besides increase of the NiO crystallite size, was observed with the increase of  $T_2$ .

We had reported the formation of dense PdO particles from a pH-adjusted  $\text{Pd}(\text{NO}_3)_2$  solution, in which

case  $\text{Pd}(\text{NO}_3)_2$  hydrolysed when the droplet was heated [6, 9]. The formation of hollow NiO particles in the present study is, however, also attributed to the nitrate precursor used for spray pyrolysis. Hydrate of  $\text{Ni}(\text{NO}_3)_2$  dissolves into its own crystalline water and liquefies above  $35^\circ\text{C}$  [13]. Therefore, it is reasonable to believe that a particle resulting from the evaporation of solvent water in the spray pyrolysis process was in fact a *droplet* of the liquefied  $\text{Ni}(\text{NO}_3)_2$  hydrate. When the decomposition gases and evaporated water were released subsequently, the liquefied particles were inflated to form a solid shell of NiO. This is a typical mechanism of the formation of hollow oxide particles by spray pyrolysis using nitrate as the starting material [5].

Similar to the NiO particles, Fig. 2c shows that Ni particles prepared at  $T_2 = 400^\circ\text{C}$  in the  $\text{H}_2\text{-N}_2$  atmosphere are also composed of nanometre-sized crystallites and have a hollow structure. However, as shown in Fig. 2d, most of the Ni particles obtained above  $T_2 = 1000^\circ\text{C}$  are dense and nearly single crystal. This indicates that densification of the particles took place above  $400^\circ\text{C}$  after Ni is formed. The similarity between the structure of Ni particles obtained at  $400^\circ\text{C}$  and the NiO particles was a result of the lack of densification within the particles.

Owing to the high melting point ( $1998^\circ\text{C}$  for NiO) and high sintering onset (about  $1300^\circ\text{C}$  for NiO) of oxides, sintering of NiO crystallites in the present preparation conditions only caused the growth of crystallites without densification of the whole particle. TGA–DTA analyses indicated that the decomposition temperature of  $\text{Ni}(\text{NO}_3)_2$  and the reduction temperature of NiO are  $300\text{--}400^\circ\text{C}$  in the present atmosphere, which is higher than the sintering onset of nanometre-sized Ni particles (about 0.3 times melting point [14], i.e.  $200\text{--}300^\circ\text{C}$ ). Therefore, Ni crystallites began to sinter immediately after the reduction of NiO. The initial sintering rate of the metal Ni crystallites yielded was very fast and just limited by the reduction rate of NiO. Deformation of the particles, which was observed in the Ni particles formed at low and medium temperatures (Fig. 3), is considered to be advantageous to the densification of the particles.

The mechanism of particle formation discussed above is illustrated schematically in Fig. 4. According to this mechanism, dense or hollow Ni particles are finally formed depending on the degree of densification, which is determined by the temperature and time at which the particles were heated. This is confirmed by the measurement of particle density, which increased

monotonously with pyrolysis temperature. The proportion of dense particles among a powder was found to increase with  $T_2$  and most particles became nearly single crystal above  $1200^\circ\text{C}$ . This result indicates that by using a sufficiently long residence time and by carefully controlling the temperature profile and gas-flow rate, most of the Ni particles can be densified below the melting point. The reason why Nagashima *et al.* obtained dense Ni particles only above the melting point of Ni is considered to be the short residence time applied in their study [8].

### 3.3. Oxidation properties of the Ni powders

It has been proved experimentally that the oxidation rate of a metal powder decreases with crystallite size and particle size. However, the crystallite sizes of the prepared Ni powders were too large to be determined and compared directly because they were approximately the same size as the particles. Therefore, we characterized the oxidation of the powders to obtain an indirect measure of the crystallinity.

TGA–DTA curves of the powders in air atmosphere are shown in Figs 5 and 6. The weight gains and exothermic peaks around  $600^\circ\text{C}$  are caused by the oxidation of Ni to NiO. The oxidation behaviour of the powders appeared to be very different; the onset and completion temperatures of oxidation varied with preparation conditions in a wide range.

For the effect of pyrolysis temperatures (Fig. 5), slopes of the TGA curves, which correspond to the

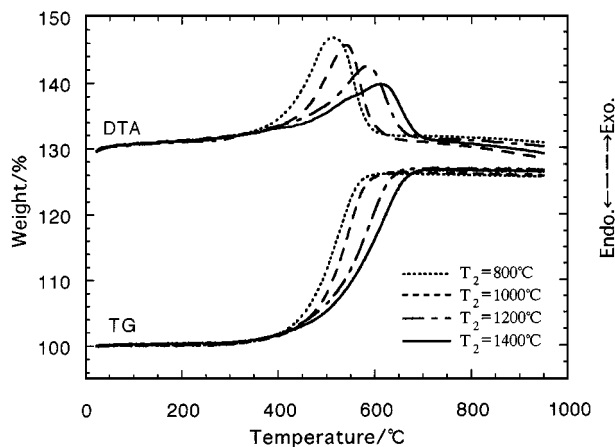


Figure 5 TGA–DTA curves of Ni powders prepared at different pyrolysis temperatures at  $T_1 = 400^\circ\text{C}$  and a carrier gas flowing rate of  $3.0\text{ cm s}^{-1}$ .

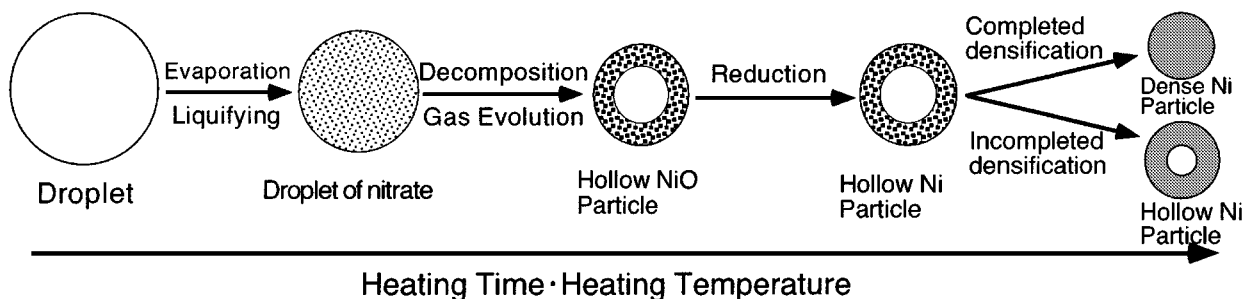


Figure 4 Formation mechanism of a Ni or NiO particle.

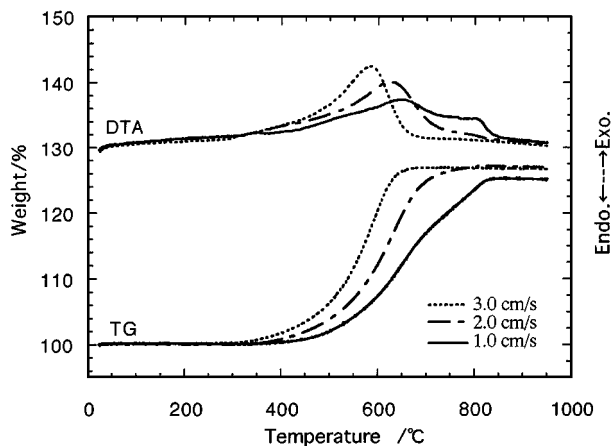


Figure 6 TGA-DTA curves of Ni powders prepared at  $T_1 = 400\text{ }^\circ\text{C}$  and  $T_2 = 1200\text{ }^\circ\text{C}$  with different carrier gas flow rates.

oxidation rates, decreased with the increase of  $T_2$ ; while the corresponding exothermic peaks in the DTA curves shifted to the high temperature side. A decrease of the oxidation rate resulted in an increase of the interval from the onset to the completion of oxidation; that weight gains and exothermic peaks became broad and flat as  $T_2$  increased.

The carrier gas flow rate, which determined the residence time of the droplets/particles in the heating zone, also had a large effect on the oxidation of the prepared powders (Fig. 6). Slower flow rates resulted in a decrease of the oxidation rate and an increase in the oxidation temperature of Ni particles. For example, Ni particles prepared at the flow rate of  $1.0\text{ cm s}^{-1}$  were even oxidized in two steps, giving out a very broad exothermic peak and flat weight gain. The onset of oxidation shifted to higher temperatures by about  $100\text{ }^\circ\text{C}$  and the completion of oxidation was above  $800\text{ }^\circ\text{C}$ , nearly  $200\text{ }^\circ\text{C}$  higher than that of  $3.0\text{ cm s}^{-1}$ .

The increase of oxidation resistance of the Ni particles resulted from improvements in crystallinity and density of the particles, which was achieved by nearly complete sintering and densification. Powders formed at higher pyrolysis temperatures and longer residence times had better crystallinity and higher density. It is reasonable to conclude from this result that a synthesis system of sufficiently high pyrolysis temperatures and a sufficiently long reaction path is necessary to prepare dense Ni particles of good crystallinity by spray pyrolysis.

#### 4. Conclusions

Dense spherical Ni particles were prepared below the melting point by the ultrasonic spray pyrolysis method. Evolution of the particle structure and the powder's oxidation property were investigated.

Drying of the droplets results in hollow spherical NiO particles in the first stage of the process. The NiO particles remain hollow in the  $\text{N}_2$  atmosphere due to a lack of sintering and densification. However, NiO is reduced above  $300\text{ }^\circ\text{C}$  in a  $\text{H}_2\text{-N}_2$  atmosphere and the Ni crystallites yielded underwent intraparticle sintering and densification subsequent to formation of a dense Ni particle. Ni powders showing a higher oxidation onset and slower oxidation rate in air were obtained by applying a higher pyrolysis temperature and a slower gas flow rate to enable complete intraparticle sintering and grain growth.

#### References

1. H. SAITO, H. CHAZONO, H. KISHI and N. YAMAOKA, *Jpn. J. Appl. Phys.* **30** (1991) 2307.
2. J. YAMAMATSU and T. NOMURA, *Funtai Oyobi Funmatsu-yakin (J. Powder Powd. Metall. Soc. Jpn)* **41** (1993) 1042.
3. K. OTSUKA, Y. YAMAMOTO and A. YOSHIKAWA, *Nippon Kagaku Kaishi* (1984) 869.
4. F. MIYOSHINO, K. SANO, K. TAKADA and F. MAKUTA, in Proceedings of the Ninth International Microelectronics Conference (IMC), Omiya, April 1996, p. 46-9.
5. G. L. MESSING, S.-C. ZHANG and G. V. JAYANTHI, *J. Amer. Ceram. Soc.* **76** (1993) 2707.
6. S.-L. CHE, O. SAKURAI, K. SHINOZAKI and N. MIZUTANI, *J. Aerosol Sci.* **29** (1998) in press.
7. T. C. PLUYM, S. M. LYONS, Q. H. POWELL, A. S. GURAV, T. T. KODAS, L. M. WANG and H. D. GLICKSMAN, *Mater. Res. Bull.* **28** (1993) 369.
8. K. NAGASHIMA, M. WADA and A. KATO, *J. Mater. Res.* **5** (1990) 2828.
9. S.-L. CHE, O. SAKURAI, K. SHINOZAKI and N. MIZUTANI, *J. Ceram. Soc. Jpn* **104** (1996) 38.
10. S.-L. CHE, O. SAKURAI, H. FUNAKUBO, K. SHINOZAKI and N. MIZUTANI, *J. Mater. Res.* **12** (1997) 392.
11. S. STOPIC, I. ILIC and P. USKOKOVIC, *Int. J. Powder Metall.* **32** (1996) 59.
12. S.-L. CHE, O. SAKURAI, A. SAIKI, H. FUNAKUBO, K. SHINOZAKI, N. MIZUTANI and K. TERAYAMA, *J. Ceram. Soc. Jpn* **105** (1997) 299.
13. A. M. GADALLA and H.-H. YU, *J. Thermal Anal.* **37** (1991) 3119.
14. M. I. ALYMOV, E. I. MALTINA and Y. N. STEPANOV, *Nanostructured Mater.* **4** (1994) 737.

Received 15 August 1997

and accepted 3 September 1998